CORE AND SHIELDING ANALYSIS OF THE SCM-100

by ***Arne P. Olson***

Advanced Accelerator Applications (AAA)
Technology Development Division

Argonne National Laboratory, Argonne, Illinois 60439
Operated by The University of Chicago for the
United States Department of Energy under Contract W-31-109-Eng-38

Report No. ANL/TD/TM02-25 and ANL-AAA-003

Report

CORE AND SHIELDING ANALYSIS OF THE SCM-100

December 21, 2001

Arne P. Olson

Advanced Accelerator Applications (AAA)
Argonne National Laboratory
9700 South Cass Avenue
Argonne, IL 60439

TECHNOLOGY DEVELOPMENT DIVISION TECHNICAL MEMORANDUM NO. TM02-25

TABLE OF CONTENTS

LIST OF FIGURES

LIST OF TABLES

ABBREVIATIONS AND ACRONYMS

ADTF	Accelerator Driven Test Facility
ANL	Argonne National Laboratory
CRBR	Clinch River Breeder Reactor
DPA	Displacements Per Atom
EBR-I	Experimental Breeder Reactor I
EBR-II	Experimental Breeder Reactor II
FFTF	Fast Flux Test Facility
IPNS	Intense Pulsed Neutron Source at ANL
LMFBR	liquid metal cooled fast breeder reactor
LMR	liquid metal cooled fast reactor
mA	milliamperes--unit of electrical or accelerator beam current
MeV	million electron volts--used to characterize accelerator beam energy or particle energy
MW	megawatt
MWt	megawatt thermal
SCM	sub-critical multiplier (a sub-critical reactor)
yr	year

EXECUTIVE SUMMARY

It is widely accepted that an intense neutron source can be produced in a suitable target by spallation neutrons generated by a high-current high-energy proton beam. Typical beam energy for such an accelerator is 400 to 2000 MeV. A conventional critical reactor can readily be replaced by a "sub-critical reactor" driven by this source. A 5 MW proton beam at 600 MeV can drive a sub-critical reactor to 100 MWt. The accelerator and the associated plant support equipment at these design specifications are complex systems, but they are well within recent technology. The purpose of this study was to examine core design and shielding design issues for a 100 MWt sodium-cooled fast-spectrum Sub-Critical Multiplier (SCM-100) based on LMFBR technology, but driven by an intense neutron source created by spallation reactions. SCM-100 is a component of the Accelerator Driven Test Facility.

In this report we provide an overview of the SCM-100 concept. Two designs were investigated:
- a vertical entry for the beam on the axial centerline;
- an inclined entry design where the core is "C" shaped and the beam enters the side of the target at an angle of 32 degrees.

A brief overview of relevant shielding design data from EBR-II is also provided. The key result of this report is that the inclined entry design cannot achieve design objectives for radial power peaking. Consequently it cannot achieve design objectives for peak neutron flux. Axial power peaking factors are controlled by the axial fuel height and the axial reflector properties. These dimensions and compositions are very similar in SCM-100 to those of EBR-II. EBR-II had an axial power peaking factor of 1.093, and a radial power peaking factor of about 1.46. The radial power peaking of SCM-100 with the inclined entry is too extreme at 2.15, and cannot be made acceptable by modifying the size and detailed shape of the "C" shaped core and reflector. The axial power peaking of SCM-100 is very close to that of EBR-II. Although these conclusions were obtained using EBR-II Mark-IIIA fuel elements of a single enrichment, they are expected to be true for any single-enrichment fuel design with a similar active fuel height and similar k-infinity.

Shielding of the grid plate was also investigated. The lower axial reflector thickness necessary to achieve the design lifetime was found to be 75 cm.

1. Introduction

It is widely accepted that an intense neutron source can be produced in a suitable target by spallation neutrons generated by a high-current high-energy proton beam. Typical beam energy for such an accelerator is 400 to 2000 MeV. The spallation reaction on heavy metal targets such as uranium, lead, tungsten, and bismuth has a threshold of about 120 MeV. The neutron yield per spallation event is almost linear, and steadily increases as the proton energy increases. Cost considerations dictate a trade-off between increasing the beam energy to get more neutrons per event, and increasing the beam current to get more events. A conventional critical reactor can readily be replaced by a "sub-critical reactor" driven by this source. The term "sub-critical assembly" historically is used in the context of zero power reactors, and is therefore not

appropriate when significant power is produced. The accelerator and the associated plant support equipment at these design specifications are complex systems, but they are well within recent technology. The purpose of this study was to examine core design and shielding design issues for a 100 MWt Sub-Critical Facility (SCF) based on LMFBR technology, but converted to use an intense neutron source created by spallation reactions. This design study assumes a 600 MeV proton beam with a power of 5 MW. Also assumed is that the SCM will be sub-critical and near $k_{effective} = 0.95$. Results presented in Section 6.2 for the inclined entry configuration show that total power predicted from neutron multiplication is about 9.5% too large in the vicinity of $k_{effective} = 0.95$. Consequently one can make a reasonable estimate that the reactivity must be slightly increased to about 0.954 in order to achieve 100 MWt when the beam power is 5.0 MW.

In this report we provide an overview of the SCM-100 concept. Two designs were investigated: one using a vertical entry for the beam on the axial centerline, and an inclined entry design where the core is "C" shaped and the beam enters the side of the target at an angle of 32 degrees A brief overview of relevant shielding design data from EBR-II is also provided. The key result of this report is that the inclined entry design cannot achieve design objectives for radial power peaking. Consequently it cannot achieve design objectives for peak neutron flux. Radial power peaking is too extreme, and cannot be made acceptable.

Shielding of the grid plate was also investigated. The lower axial reflector thickness necessary to achieve the design lifetime was found to be 75 cm.

2. SCM-100 Concept

2.1 Overview

The SCM-100 is an advanced research facility with capabilities to study the performance of new reactor core and fuel concepts under conditions of sub-criticality and driven by an intense neutron source [1]. It is designed to operate in steady state at up to 100 MWt. The design objectives regarding peak neutron flux and power density are closest to those of Liquid-Metal cooled Fast Breeder Reactors (LMFBR), which have been studied intensively since EBR-I began operation at ANL-West in 1951. EBR-II design followed in the late 1950's [2]. Much of what was learned from EBR-I and EBR-II is applicable to the SCM-100, because the same concept of a pool-type facility cooled by sodium applies.

Differences between EBR-II and the SCM-100 are:

1 The core is not operated anywhere near critical; the neutron population is maintained at a stable level as a response of sub-critical multiplication to the spallation neutron source.
2. The accelerator is unlikely to be as reliable as have conventional critical reactors in providing neutrons continuously over extended periods of time.
3. The neutron flux spectrum leaving the target has a very hard component of about 1.5% of the neutrons, whose energies range above 20 MeV and extend to 600 MeV.
4. The fission products caused by spallation extend over the entire periodic table below the target isotopes.

5. A reactor control system in the conventional sense will not be needed, but slow-acting long-term reactivity control will be needed to compensate for burnup and to maintain sub-criticality during shutdown.

Common features of the SCM-100 and EBR-II are:

1. Initial core has same Mark-IIIA fuel element, with an active fuel height of about 35 cm, and identical composition upper and lower neutron reflectors (reflector heights to be determined by shielding needs). The fuel design of later cores will be progressively switched to a new design ("ATW fuel") to demonstrate waste transmutation.
2. Same coolant of sodium, and similar operating temperatures.
3. Tank type design (no external loops). The heat exchanger is inside the tank but sufficiently far away from the core to not activate the secondary coolant beyond a design limit.
4. Similar core support plate design.
5. Similar design of rotating plugs for access to the core, heat exchanger, and pumps.

2.2 Details of the Core Designs

The fuel region in the multiplier assembly for the vertical entry is surrounded by reflector assemblies to fit within a 121.92 cm diameter envelope inside the multiplier vessel, inside the primary vessel. The annular region between this envelope and the vessel is filled with fast neutron shielding and moderator. The multiplier core consists mostly of hexagonal fuel assemblies similar to EBR-II Mk-3 units. The assemblies measure 5.74 cm across flats and contain 61 U-10%Zr fuel rods 5.84 mm in diameter mounted on a 6.91mm triangular pitch with a 34.29 cm-long fuel column. About 90-110 fuel assemblies are necessary in order to generate 95 MWt from the core, provided that the radial power distribution is quite flat. The proton target will provide an additional 3.7 MWt. Early in the SCM-100 core design process, provision for three test loops was envisioned but later deleted.

As indicated in Section 2.1, there are two core designs of interest, shown in Figs 2.1 and 2.2. The first requires a proton beam delivered to the top of the SCM-100, entering it from above, vertically downward, on the core axial centerline. The second requires a proton beam delivered to the top of the SCM-100, entering it from above, inclined at 32 degrees to the core axial centerline.

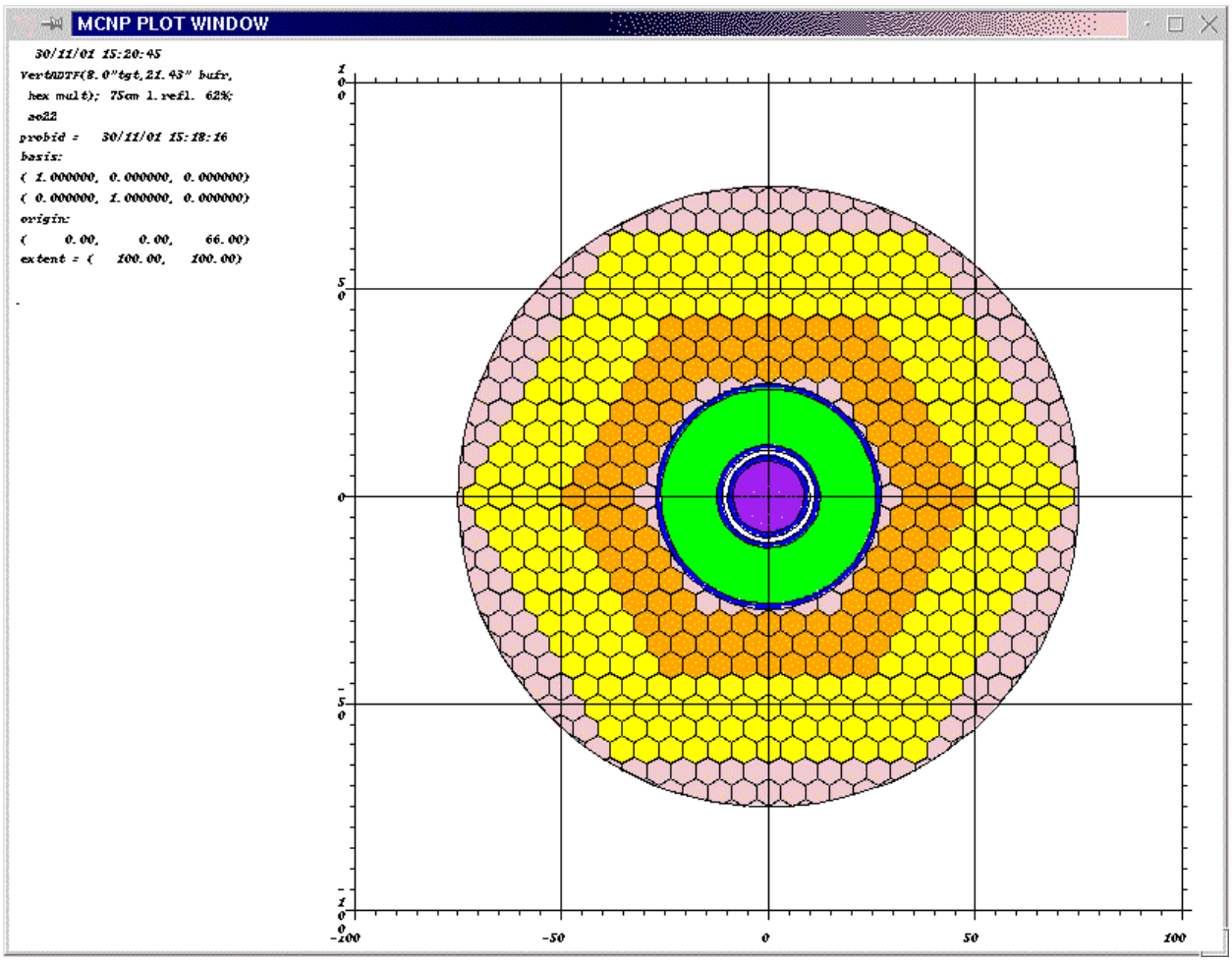

Figure 2.1 MCNPX Vertical Entry Model for SCM-100 using 126 Mk-IIIA Fuel Assemblies

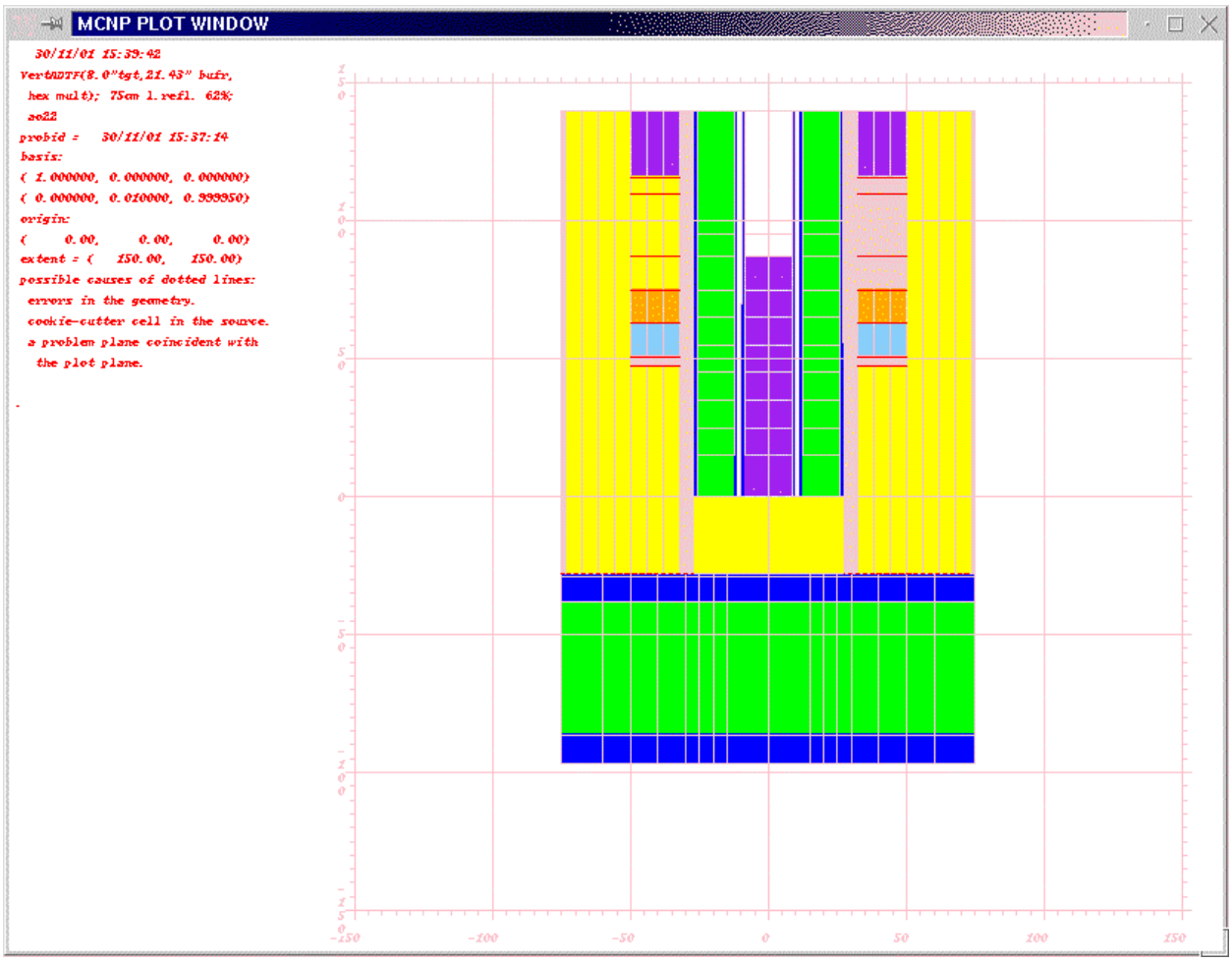

Figure 2.2 Vertical-Entry SCM Target and Multiplier, Horizontal Section

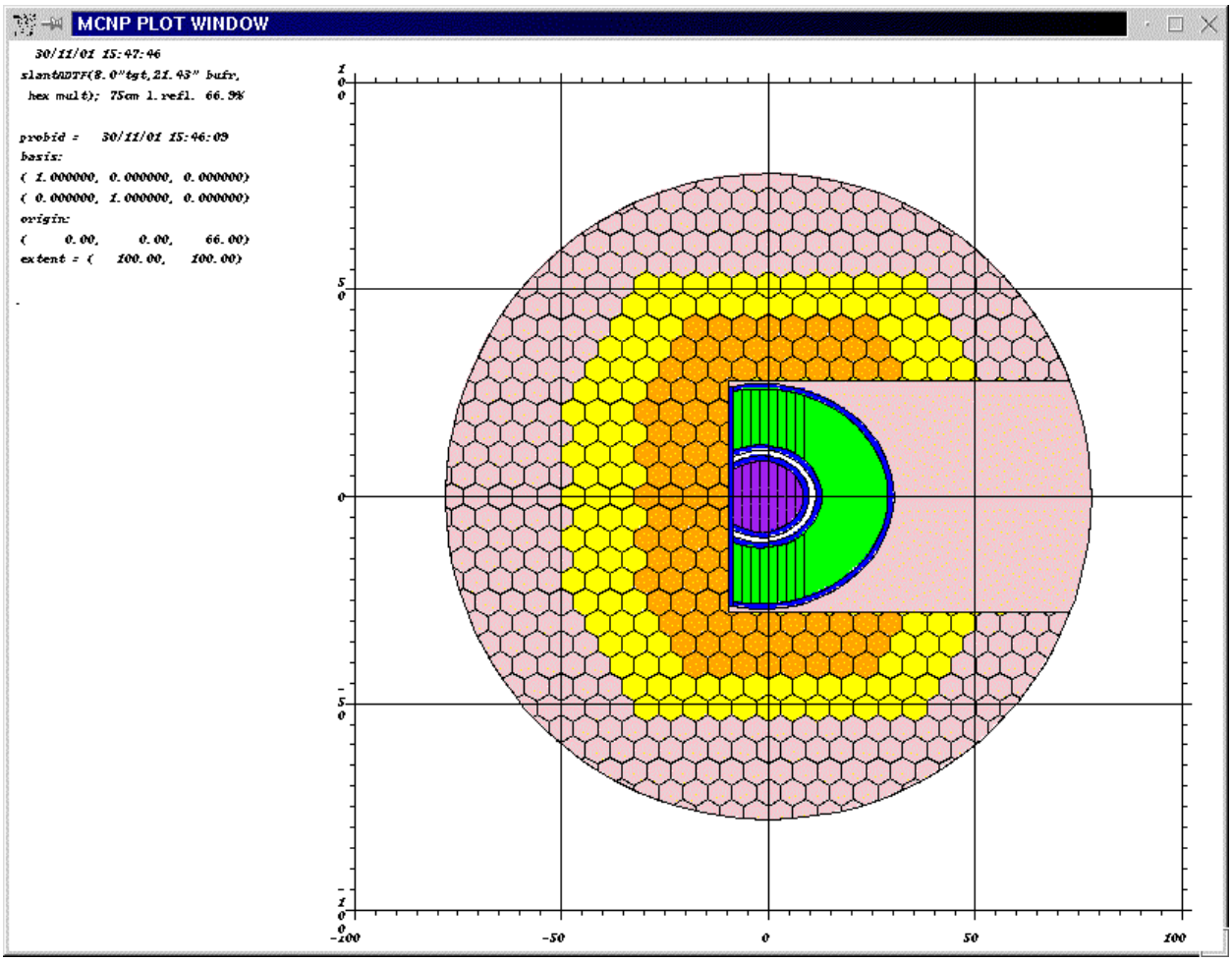

Figure 2.3 Inclined-Entry SCM Target and Multiplier, Horizontal Section

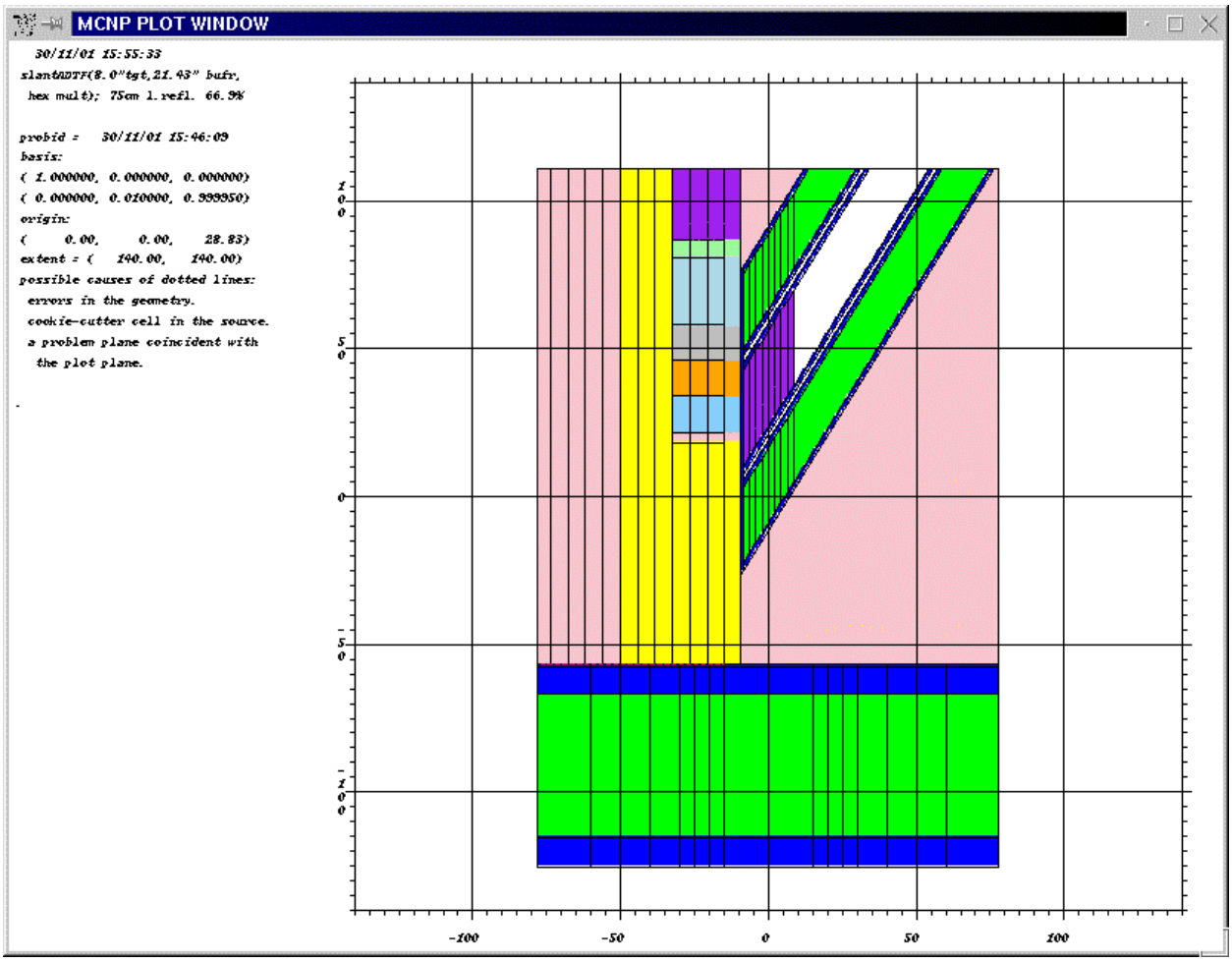

Figure 2.4 Inclined-Entry SCM Target and Multiplier, Vertical Section

3. Historical Shield Design Information from EBR-II

3.1 Historical Guidance: Design Needs for EBR-II and Other LMR's in Relation to the SCM-100

What were the shielding needs for the EBR-II and for similar fast reactors such as FFTF, CRBR, PFR, and PHENIX? Work by S.A. Kamal [3], and by Grotenhuis, McArthy, and Rossin [4] was examined for insights and key concerns.

The purpose of the radial shields is to attenuate the neutron and gamma-ray fluxes, thereby reducing the radiation damage to and activation of structural components. A pool reactor such as EBR-II and the present ANL concept for the SCM-100 have the intermediate heat exchangers (IHX) inside the primary tank, while loop-type reactors have the IHX outside the tank. It is important to note that the secondary loop sodium is activated by primary neutron capture to Na^{24}, which has about a 15 hr half-life. Na^{24} emits both beta and gamma radiation, which is an issue for personnel radiation dose acquired during operation and maintenance. The main concern for EBR-II shielding design was the secondary loop sodium activation. This also is a key design issue for the SCM-100.

Radial reflectors (sometimes called removable radial shields, if they are built from components that can be installed on the grid plate like fuel assemblies) for fast reactors have been made of materials compatible with sodium such as type 304 stainless steel, type 316, or Inconel 600. The nickel content of these materials is 8-11% for 304, 10-14% for 316, and more than 72% for Inconel 600. As the nickel content increases, the neutron reflectiveness increases.

Shield materials used in LMR's included graphite, iron, stainless steel, and boron carbide. The graphite, iron, and boron carbide must be clad in stainless steel.

The EBR-II shield used graphite to which was added 3 weight % boron carbide. The IHX in EBR-II was protected by a borated steel shell, 1.5% boron, nominally 2.54 cm thick. It is reasonable to assume that a similar protective layer will be necessary for the IHX in the ADTF.

The design neutron flux levels in EBR-II, FFTF, and CRBR are given by Kamal [3], and by Fryer *et al.* [5]. For purposes of the ADTF, the EBR-II values of interest are:

Maximum total flux in core	3.55×10^{15} n/cm^2-s
Maximum flux >0.1 MeV at reactor vessel(outer shell)	9.0×10^{11} n/cm^2-s
Maximum flux >0.1 MeV at primary tank wall	8.6×10^{4} n/cm^2-s
Maximum slow flux <0.27 eV in the IHX with borated steel shell	3×10^{5} n/cm^2-s
Secondary sodium coolant activity at 62.5 MWt	5.4×10^{-8} Ci/cm^3
Maximum fast neutron fluence in row 1 of grid plate (at 40 years)	1.6×10^{22} n/cm^2

For FFTF and CRBR, the main concern was ensuring 10% residual ductility for permanent components (some FFTF components were designed to 5%). It is pointed out in [4] that the austenitic steels used in liquid metal cooled reactors have high initial ductilities. The integrated neutron doses required to achieve embrittlement saturation are not reached at reactor vessel locations over the lifetime of a liquid-metal-cooled system. Core barrel welds in CRBR were limited to 1.1 x 10^{22} n/cm^2, equivalent to 15.7 x 10^{12} n/cm^2-s, while the vessel was limited to 6 x 10^{11} n/cm^2-s.

Material fluence limits used in the final design of CRBR are also given by Kamal [3]:

SS316	3.5 x 10^{22} n/cm^2
SS304	1.8 x 10^{22} n/cm^2
SS308	1.1 x 10^{22} n/cm^2

For SCM-100 design purposes, these values can be used as a guide but the presence of very energetic neutrons from spallation (not in CRBR) probably will alter significantly these limits. Once the neutron spectrum is known at key locations, these limits should be reassessed. A literature search should be made of recent irradiation work on materials properties when subjected to high-energy spallation neutrons. This will guide setting realistic fluence limits. It is worth noting that for CRBR, the core barrel welds were limited to a maximum fluence of 1.1 x 10^{22} n/cm^2.

Measurements on ten irradiated subassemblies began in EBR-II in 1965. These subassemblies, known as SURV-1 through SURV-10, were periodically removed and examined. Results reported for SURV-8 [5] showed that a maximum fluence of 2.7 x 10^{22} n/cm^2 was reached in SS-304 while retaining 17% residual ductility. The irradiation was carried out nominally at 370 C. This residual ductility is very high compared with the FFTF and CRBR design limits, thus assuring that EBR-II SS-304 components could perform well over a life extension to 40 years.

Proton Beam Tube

For the proton beam tube wall, the ANL IPNS Upgrade Project [6] assumed a beam fractional energy loss per unit length which activated the wall. A simple correlation was used to estimate the radiation dose rate after shutdown, which in turn yielded information about personnel dose rates during maintenance. This same approach can be used for the shielding analysis of the SCM-100, for portions of the beam tube wall which are far from the reactor vessel. For the angled proton beam entry design, welds at the junction of the beam tube/vessel wall should be assessed against fluence limits in order to assure that the weld lifetime is adequate.

Shielding Interface

Shielding design inputs are: physical arrangement, dimensions, compositions, and temperatures of all components within the vessel, and outside the vessel to outside of the biological shield. It also requires input concerning design lifetimes of key components. Furthermore, it requires information on materials limits from irradiation by neutrons in a hard neutron spectrum similar to that of LMR's. Lastly, personnel dose rate limits and design basis occupancy time limits will need definition for all portions of the ADTF which can be reached for operation and maintenance.

Output from the shielding analysis will iteratively guide the choice of materials, thicknesses, and arrangements of shielding materials, in order to converge on a workable design that satisfies the design limits.

Shielding Analysis Process

The impact on shielding components caused by neutrons above 20 MeV needs to be assessed and compared to the impact caused by neutrons below 20 MeV. This can be done by using the MCNPX code (Version 2.1.5) [7] to account for all neutron energies, including the very high energy neutrons, and by using multigroup transport and diffusion theory codes such as DANTSYS and DIF3D for simplified analysis. In cases where the fraction of neutrons above 20 MeV is quite small, this may permit careful application of conventional multigroup diffusion and transport theory methods for neutron and photon transport.

4. Shielding Studies for Damage to the Grid Plate

Shielding analysis of damage to the grid plate was performed using the MCNPX code. The basis for the calculation was the MCNPX model created by John Stillman for the vertical entry configuration of the SCM-100 (100 MWt, with 5 MW beam power). It is concluded that a lower axial reflector thickness of 75 cm (85% steel, 15% sodium) will yield 3.0 DPA/fpy at a total power of 100 MWt and 100% capacity factor.

4.1 Modeling

The model contains the subcritical multiplier as a hexagonal array of homogenized subassemblies. Grid plates and lower plenum were added. The beam was assumed to be of 10.16 cm radius. The target was of Pb-Bi, 10.643 cm radius, inside an ss-316 beam tube of 11.913 cm outer radius, and inside a Pb-Bi buffer out to 27.216 cm radius. A hexagonal multiplier of ~120 subassemblies is used. The entire system is contained within a 75 cm radius tank of sodium.

In the axial dimension, the model has a 10.16 cm thick lower grid, a 48.26 cm thick sodium plenum, a 10.16 cm thick upper grid, and a 100 cm thick lower reflector (80% ss-316, 20% sodium). There is a 3.44 cm thick section between the top of the reflector and the bottom of the fuel. The Fuel is U-10Zr, 36.66 cm in height. A fission gas plenum is above the fuel, 22.65 cm in height. There is a 5.81 cm thick layer between the fission gas plenum and the bottom of the upper reflector, which is 24.08 cm thick. There is nothing in the model above the upper reflector, or outside a 75 cm radius, or below the lower grid. Particles that reach those boundaries escape.

For purposes of calculating radiation damage to the upper grid plate, a series of radial annuli were defined for the top 1 cm thickness. The radii are: 0-15, 15-20, 20-25, 25-30, 30-40, 40-60, and 60-75 cm. The area-averaged effective radii are: 10.61, 17.68, 22.64, 27.61, 35.36, 50.99, and 67.91 cm.

The cases studied are given in Table 4.2. It should be noted that the target and buffer in an initial model (Cases C.1-C.4) extend to the limit of the axial reflector. The model used in Case C.5 has the target and buffer ending at the level of the bottom of the active fuel.

4.2 Results & Conclusions

The radiation damage (displacements per atom) to the grid plate will be peaked at the center, under the target. Because the system has a strong source, the damage has two components: one from the target, depending on beam power, and the other from the subcritical multiplier, depending upon the power generated in it. Displacement rates cannot be directly scaled with system power, but do scale roughly as

$$\text{dpa} = A(\text{Power in SCM}) + B,$$

where A and B are constants determined by a particular configuration where the only change is the fuel enrichment to adjust total power.
There is no need to have the central portion of the grid plate solid, since there will be no multiplier locations near the center of the subcritical multiplier. Even so, it is instructive to consider the dose rate to iron in the top 1cm thickness of the upper grid plate, as a function of radius. I assumed that the target delivered 600 MeV protons in a beam of 8.31 mA, or 1.6356×10^{24} p/year at 100% capacity factor. Tally data for iron displacements per atom were obtained from Y. Gohar (private communication). Table 4.1 displays the results for the above system (larger beam diameter than now desired; fuel enrichment 67.18% also larger than desired, producing too much power).

Table 4.1 DPA to Iron for 100 cm Lower Reflector (80% steel)

Top 1 cm thickness of Upper Grid Plate
System total power = 248 MWt at $k_{eff} = 0.9798 \pm 0.0007$

Radius, cm	DPA/yr (100% c.f.)	Lifetime for 3 DPA, yr (5 Mw target, 80% c.f.)
10.61	0.1975 ± 2.0%	19.0
17.68	0.1675 ± 2.0%	22.4
22.64	0.1453 ± 1.9%	25.8
27.61	0.1271 ± 1.8%	29.5
35.36	0.0882 ± 1.7%	42.5
50.99	0.0406 ± 1.6%	92.4
0.0139 ± 2.1%	270	

At an effective radius of 10.61 cm, only 1.1% of the DPA from neutrons was due to neutrons with energies > 16 MeV. DPA from protons was also calculated. It is effectively zero (0.00005 DPA/yr), as almost no protons arrived at the upper grid plate.

These results required refinements in the beam diameter (to match the desired 40 μ-amp/cm^2) and enrichment, to reduce the power. The k_{eff} was reduced by reducing the fuel enrichment. Table 4.2 contains DPA results for other configurations.

Table 4.2 DPA to Iron for 105 cm Lower Reflector (80% steel)

Top 1 cm thickness of Upper Grid Plate

Case description	Fuel w/o, %	P, MWt	Central DPA/fpy
C.1 10.16 cm beam target and buffer too long	67.18	248.	0.146 ± 2.3%
C.2 10.16 cm beam target and buffer too long	60.0	71.2	0.0555 ± 8.3%
C.3 10.16 cm beam target and buffer too long	62.0	91.1	0.0796 ± 9.1%
C.4 8.143 cm beam target & beam extend to bottom of fuel; large gap between beam tube/buffer	62.0	87.9	0.134 ± 7.7%
C.5 8.143 cm beam target & beam extend to bottom of fuel, reduced gap between beam tube/buffer	62.0	95.0	0.0261 ± 5.8%

Case C.5 is the most reliable result. It is geometrically correct, and has the correct enrichment to produce nearly 100 MWt. Scaling exponentially with thickness consistent with results from Y. Gohar yields an estimated thickness of 75 cm at 85% steel will yield 3.0 DPA/fpy. The other cases provide insight into how important other design details are in determining the shielding thickness. These results suggest that the height, diameter, wall thickness, and gap dimensions of the buffer relative to the fuel and target all affect not only core physics, but also the damage to the grid plate. Gas production rates from hydrogen and helium were obtained for the upper portion of the lower support plate, for the vertical-entry sub-critical multiplier containing 126 fuel assemblies, and using the Pb-Bi target design.

5. Inclined Entry Design

5.1 Modeling of the Core

The 32 degree inclined entry beam configuration was modeled in MCNPX using a similarly-dimensioned Pb-Bi target and buffer. The target itself was shaped like a rhombus in elevation, and was arranged to have its geometrical center at the geometrical center of the fuel as in the vertical entry design. Some slight shifting of the target center may be necessary for reducing power peaking effects (to place the neutron source center most effectively). For this more

complex geometry, it was necessary to perform stochastic numerical integration in order to obtain the volumes of many cells in the model. The procedure was worked out and verified using simple test cases for which the actual volumes were known. The inclined source specification was established and verified in a simplified model where all cells were void. Proton currents through surfaces were edited to prove that the beam was correctly oriented and confined. This modeling effort for the inclined beam geometry can now be simply utilized for other target designs.

A variety of "C" shaped core layouts were studied in order to see if a power of 100 MWt could be achieved. A reasonable core layout with 98 fuel assemblies (standard EBR-II Mk-III) was created. This configuration will require a steel-sodium reflector element below the beam tube on the open side of the "C." For present survey purposes, pure sodium was used. It was found, as shown in Table 5.1, that this neutronically leaky core could provide the necessary thermal power. Power peaking effects and peak flux performance have not been determined. These results suggest that reactivity compensation for burnup losses could be accomplished by periodically increasing the reflector size, rather than by increasing the core size, which would undesirably reduce the core average power density.

Table 5.1 Effect of Radial Reflector Size on Power

Target fixed at 5 MWt, and 98 fuel assemblies

Description of Radial Reflector	*Number of Radial Reflector Elements*	*Power, MWt*
No radial reflector	0	29.69
1 row on three sides of "C"	41	48.41
2 rows " " " " "	84	78.46
3 rows " " " " "	135	120.5

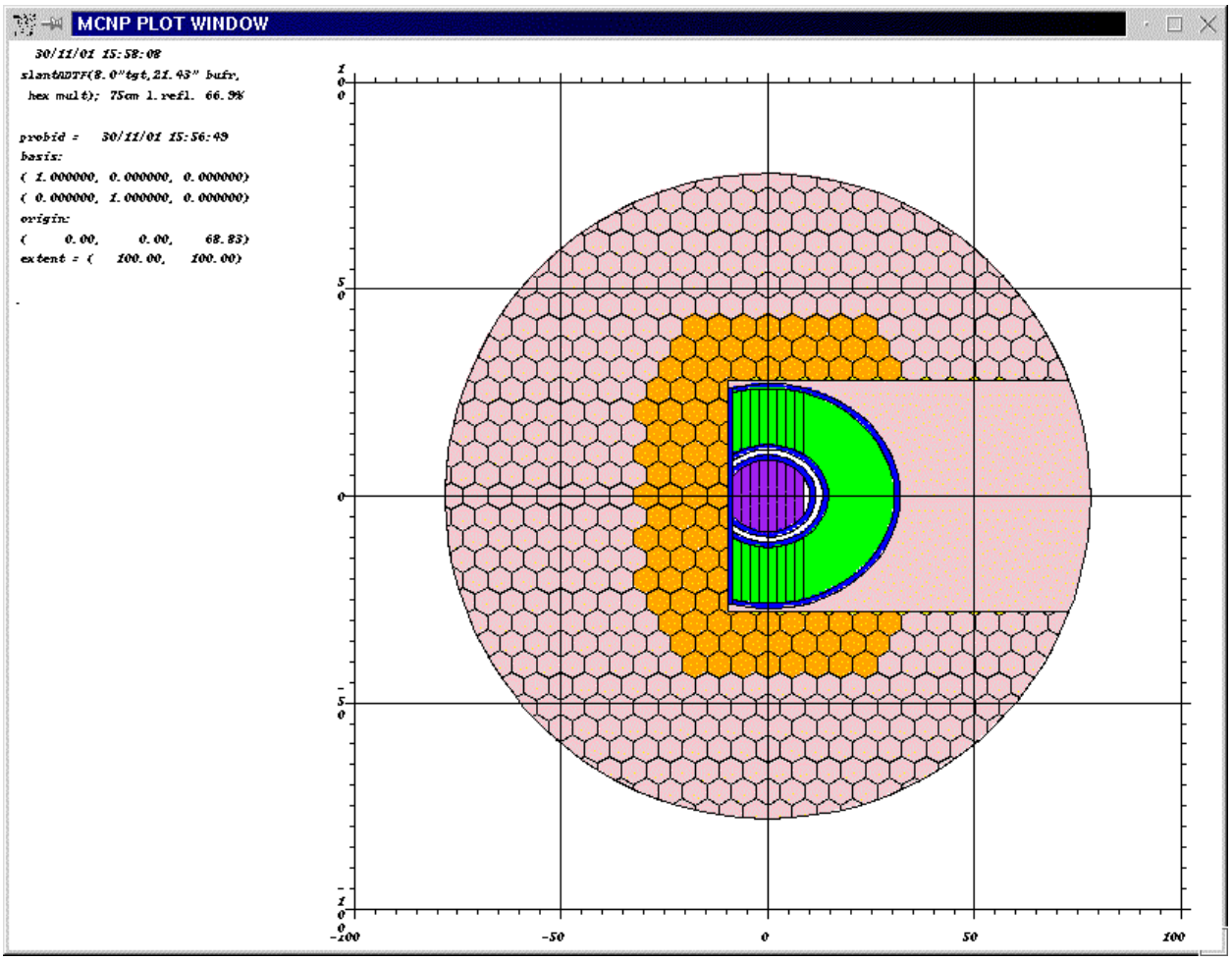

Figure 5.1 MCNPX Inclined Entry Model for SCM-100 using 98 Mk-IIIA Fuel Assemblies and No Reflector Assemblies

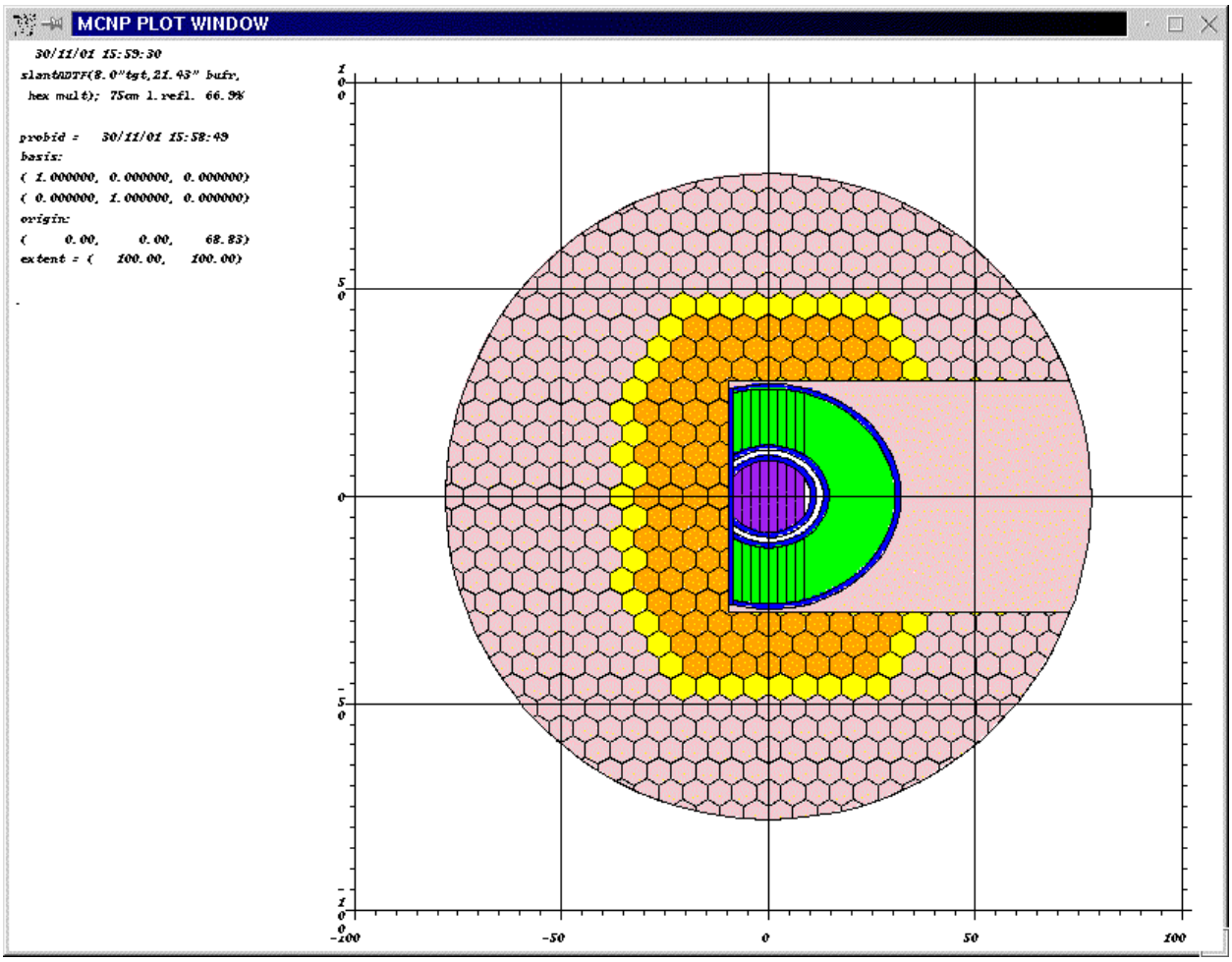

Figure 5.2 MCNPX Inclined Entry Model for SCM-100 using 98 Mk-IIIA Fuel Assemblies and 41 Reflector Assemblies

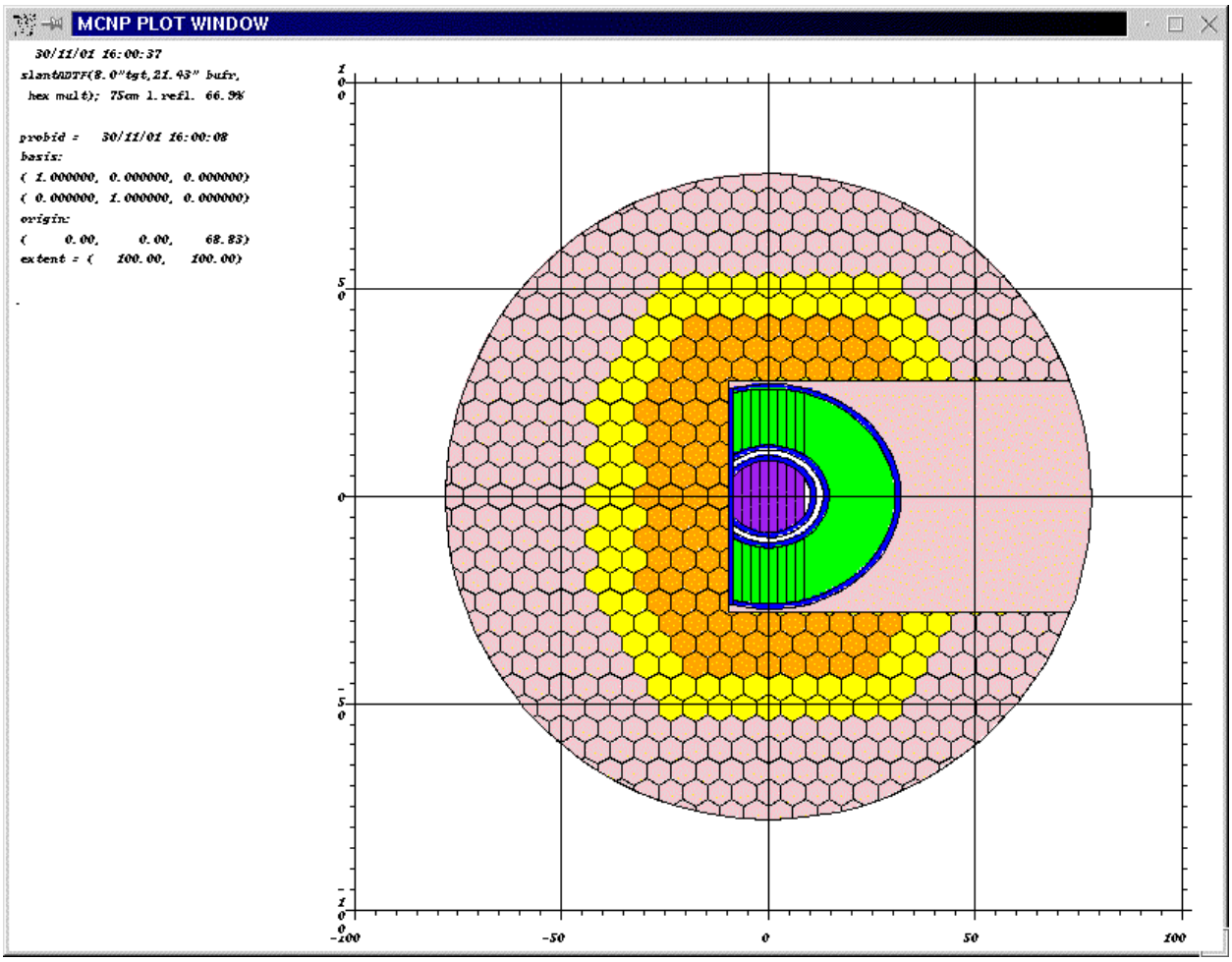

Figure 5.3 MCNPX Inclined Entry Model for SCM-100 using 98 Mk-IIIA Fuel Assemblies and 84 Reflector Assemblies

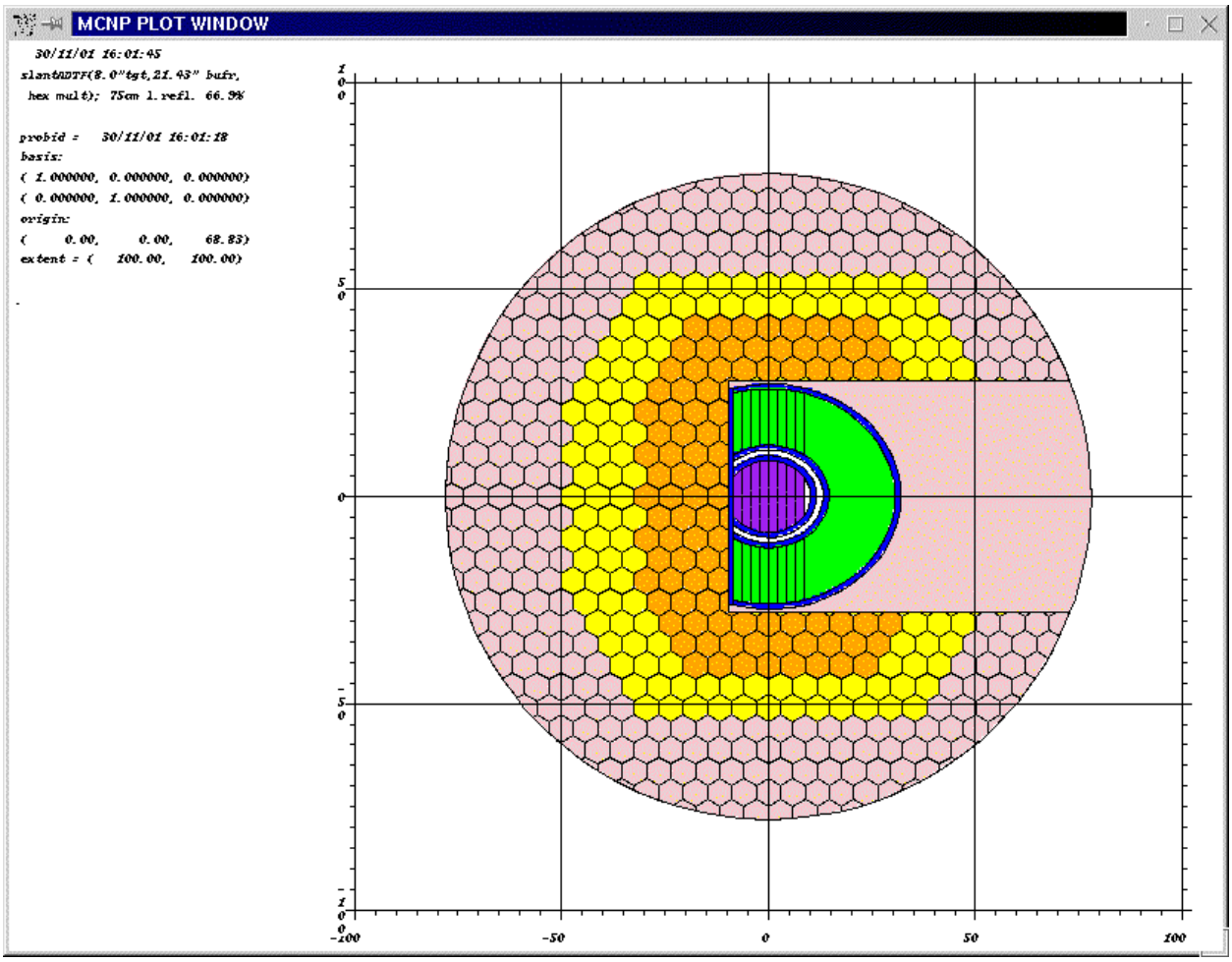

Figure 5.4 MCNPX Inclined Entry Model for SCM-100 using 98 Mk-IIIA Fuel Assemblies and 113 Reflector Assemblies

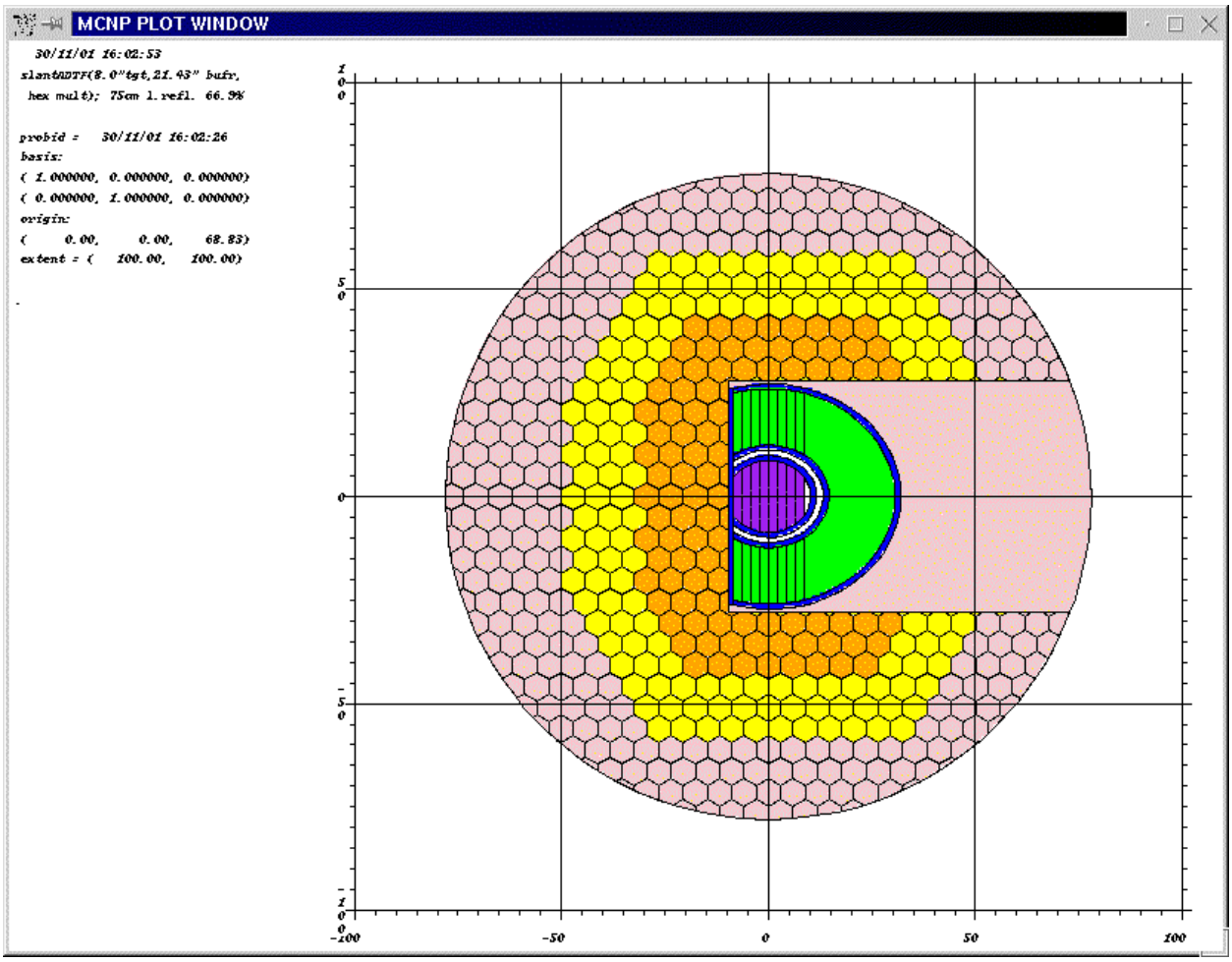

Figure 5.5 MCNPX Inclined Entry Model for SCM-100 using 98 Mk-IIIA Fuel Assemblies and 135 Reflector Assemblies

5.2 Neutron Spectrum Calculations

We have estimated the neutron flux at the Subcritical Multiplier (SCM-100) station of the Accelerator-Driven Test Facility (ADTF). Only a preconceptual design of the facility has been completed at this time. Therefore, the values provided must be treated as very preliminary as they are likely to change as the multiplier design evolves. Nevertheless, the values still provide a relative estimate of the high-energy tail of the neutron flux spectrum.

The following spectrum has been calculated using an MCNPX model of a liquid lead-bismuth target and a 126-assembly multiplier. The assemblies are of the EBR-II Mk-III design. The calculations have been carried out for the neutron spectrum outside the buffer, at core center. A vertical insertion configuration for the beam transport tube in the multiplier has been used.

The following data are the derived neutron spectrum from a neutron flux edit at the surface of the buffer.

E(upper), Mev	Flux, n/cm^2-s
1.5840E-03	5.11260E-04
2.5120E-03	2.63591E-04
3.9810E-03	1.51227E-04
6.3100E-03	2.87268E-04
1.0000E-02	4.40798E-04
1.5840E-02	7.79693E-04
2.5120E-02	1.46181E-03
3.9810E-02	1.51572E-03
6.3100E-02	2.51678E-03
1.0000E-01	3.64380E-03
1.5840E-01	5.33137E-03
2.5120E-01	6.26502E-03
3.9810E-01	8.59449E-03
6.3100E-01	8.66912E-03
1.0000E+00	6.57542E-03
1.5840E+00	5.20429E-03
2.5120E+00	3.38908E-03
3.9810E+00	1.75846E-03
6.3100E+00	6.85634E-04
1.0000E+01	1.54868E-04
1.5840E+01	2.38411E-05
2.5120E+01	1.42208E-05
3.9810E+01	1.40534E-05
6.3100E+01	1.19591E-05
1.0000E+02	9.80680E-06
1.5840E+02	6.23137E-06
2.5120E+02	2.97548E-06
3.9810E+02	7.07982E-07
6.0000E+02	2.84092E-08

The total flux is 5.82835E-02 n/cm^2-s per source proton. One can scale this result by 5.201E+16 to yield a total flux of 3.03E+15 n/cm^2-s at a total power of 95.41 MWt (5.0 MW in the beam). The statistical errors (standard deviation) are 0.4 to 1% up to 10 MeV, less than 2% up to 100 MeV, and less than 4% up to 251 MeV. The last two points are poorly defined at 12% and 100%.

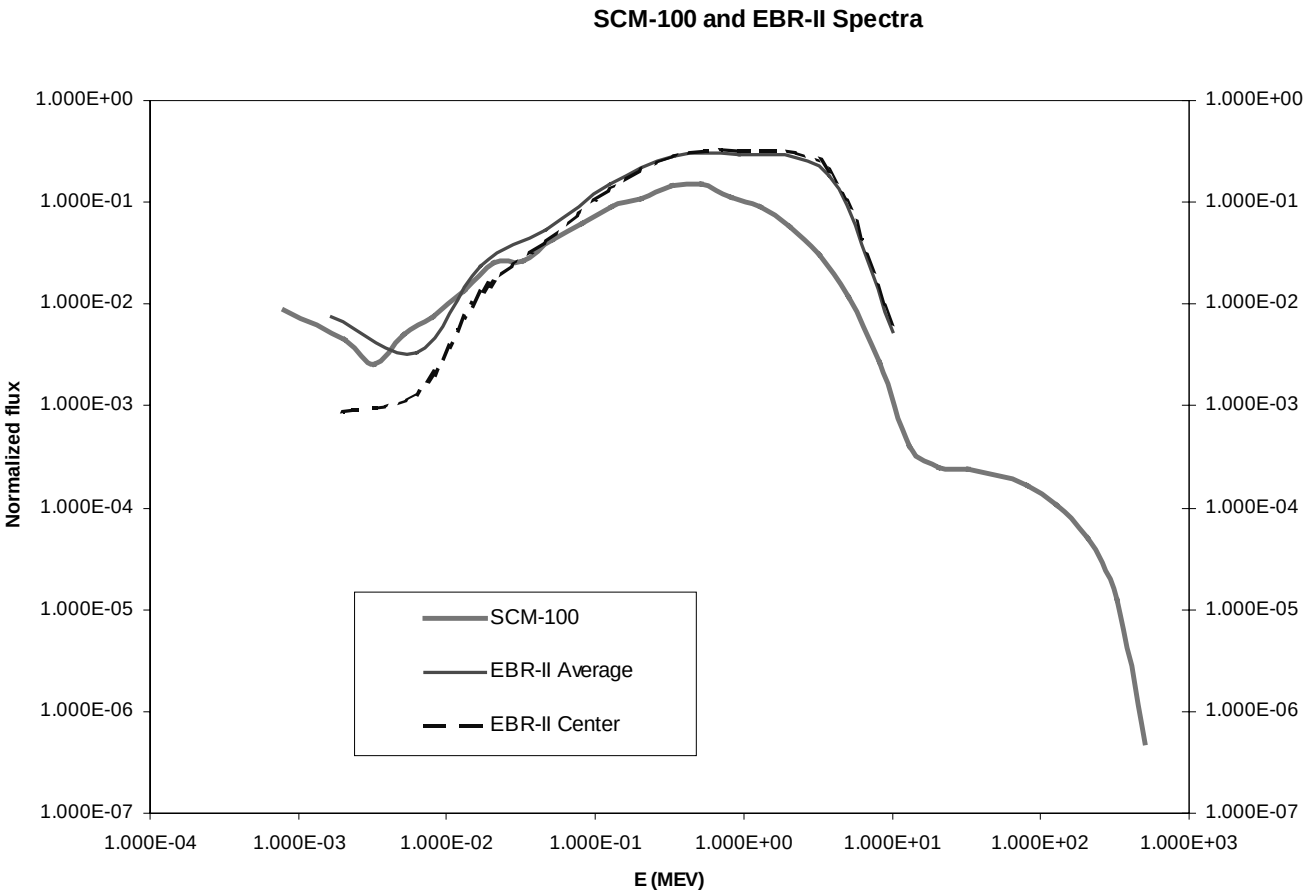

Figure 5.6 Neutron Spectrum EBR-II vs. SCM-100

5.3 Typical EBR-II Spectrum

For comparison, John Stillman (ANL, Private Communication) has estimated the EBR-II spectrum using the DIF3D code. The DIF3D model is for a problem consisting of 6 full rows of Mk-III driver assemblies (the same assembly type used in the SCM-100 model). k_{eff} is 1.0932. Results in the central hex location (at the core midplane) and averaged over the core are as follows:

	Flux/Total-flux	
E-max (eV)	Core center	Core average
1.42E+07	0.00627	0.00544
6.07E+06	0.20602	0.18149
1.35E+06	0.31211	0.29082
4.98E+05	0.28265	0.28233
1.83E+05	0.13753	0.15182
6.74E+04	0.04072	0.05321
2.48E+04	0.01252	0.02402
9.12E+03	0.00134	0.00330
3.35E+03	0.00084	0.00757

The core average total flux is 1.93778e+15 n/cm^2/s (total power=63 MW, as in EBR-II).

The SCM-100 and EBR-II spectra are compared in Figure 5.1.

5.4 Neutron Spectrum at Various Radial Locations in the SCM-100

The neutron spectrum has been calculated using an MCNPX model of a liquid lead-bismuth target and a 126-assembly multiplier. The assemblies are of the EBR-II Mk-III design. The calculations have been carried out for the neutron spectrum at core center. A vertical insertion configuration for the beam transport tube in the multiplier has been used.
The following data are the derived neutron spectrum from a neutron flux edit at the outside surface (on one flat) of rings 7-9. Ring 7 is the inner fuel ring, 8 is the middle fuel ring, 9 is the outer fuel ring.

Ring 7: Outer surface of First Fuel Ring		Ring 8: Outer surface of Middle Fuel Ring	Ring 9: Outer surface of Middle Fuel Ring
E(upper), MeV	Flux, n/cm^2-s	Flux, n/cm^2-s	Flux, n/cm^2-s
1.5840E-03	3.734E-05	3.728E-05	1.544E-05
2.5120E-03	1.877E-05	2.760E-05	7.061E-05
3.9810E-03	1.353E-05	1.141E-05	3.273E-05
6.3100E-03	5.077E-05	5.080E-05	8.531E-05
1.0000E-02	1.090E-04	9.321E-05	1.181E-04
1.5840E-02	2.599E-04	2.028E-04	2.110E-04
2.5120E-02	5.236E-04	4.939E-04	5.761E-04
3.9810E-02	5.780E-04	4.673E-04	4.457E-04
6.3100E-02	9.801E-04	8.604E-04	7.623E-04
1.0000E-01	1.550E-03	1.353E-03	1.134E-03
1.5840E-01	2.345E-03	2.104E-03	1.708E-03
2.5120E-01	2.921E-03	2.557E-03	2.003E-03
3.9810E-01	4.204E-03	3.635E-03	2.944E-03
6.3100E-01	4.529E-03	3.887E-03	2.964E-03
1.0000E+00	3.616E-03	3.314E-03	2.467E-03
1.5840E+00	3.214E-03	2.914E-03	2.033E-03
2.5120E+00	2.392E-03	2.204E-03	1.531E-03
3.9810E+00	1.473E-03	1.423E-03	9.143E-04
6.3100E+00	6.330E-04	6.110E-04	4.184E-04
1.0000E+01	1.484E-04	1.300E-04	8.659E-05
1.5840E+01	1.622E-05	1.478E-05	8.379E-05
2.5120E+01	7.000E-06	3.376E-06	2.004E-06
3.9810E+01	5.343E-06	3.560E-06	1.925E-06
6.3100E+01	6.075E-06	3.222E-06	1.867E-06
1.0000E+02	5.136E-06	2.626E-06	1.546E-06
1.5840E+02	2.656E-06	1.360E-06	7.071E-07
2.5120E+02	1.089E-06	4.461E-07	4.482E-07
3.9810E+02	3.815E-07	2.054E-07	9.165E-08
6.0000E+02	0.000E-00	0.000E-00	0.000E-00

The total flux in Ring 7 is 2.964E-02 n/cm^2-s per source proton. One can scale this result by 5.201E+16 to yield a total flux of 1.541E+15 n/cm^2-s at a total power of 95.41 MWt (5.0 MWt in the target). The statistical errors are up to 5% up to 10 MeV, about 14% up to 100 MeV, and less than 30% up to 251 MeV. The last two points are poorly defined.

Similarly, the total flux in Ring 8 is 2.641E-02 n/cm^2-s per source proton. One can scale this result by 5.201E+16 to yield a total flux of 1.374E+15 n/cm^2-s at a total power of 95.41 MWt (5.0 MWt in the target). The statistical errors are up to 5% up to 10 MeV, about 20% up to 100 MeV, and less than 19% up to 158 MeV. The last three points are poorly defined. The total flux in Ring 9 is 2.068E-02 n/cm^2-s per source proton. One can scale this result by 5.201E+16 to yield a total flux of 1.076E+15 n/cm^2-s at a total power of 95.41 MW (5.0 MWt in the beam). The statistical errors are up to 5% up to 10 MeV, about 24% up to 100 MeV, and less than 45% up to 251 MeV. The last two points are poorly defined.

Additional data is available for the ring 10 location, in the first reflector ring.

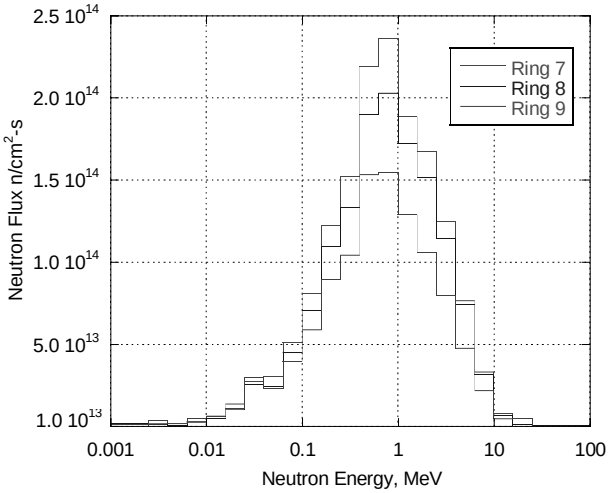

Figure 5.7 High-Energy Portion of Neutron Spectrum

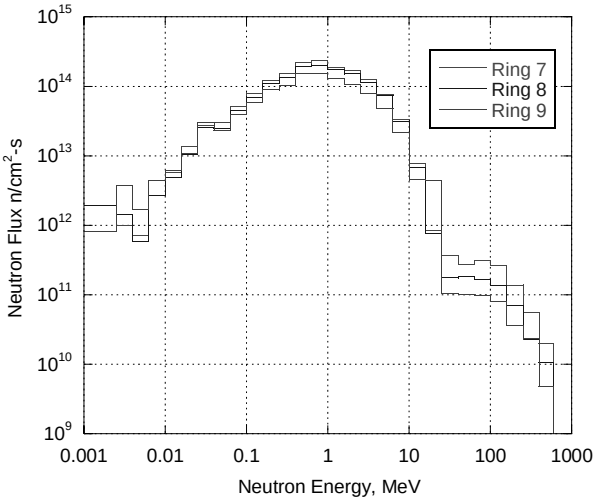

Figure 5.8 Low Energy Portion of Neutron Spectrum

6. Inclined Entry Core and Target Arrangement Study

6.1 Core Arrangement

The 32 degree inclined entry beam configuration was modeled in MCNPX using a Pb-Bi target and buffer. The target itself was shaped like a rhombus in elevation, and was arranged to have its geometrical center at the geometrical center of the fuel as in the vertical entry design. Some slight shifting of the target center is necessary to reduce power peaking effects (to place the neutron source center most effectively), or to maximize the power production of the system. A base case of 98 fuel assemblies and 113 reflector assemblies was studied by varying the location of the intersection of the beam axis with the core axis. The z-value was varied over a range from –4 to +6 cm, as shown in Table 1.
A variety of "C" shaped core layouts were studied in order to see if a power of 100 MWt could be achieved. A reasonable core layout with 98 fuel assemblies (standard EBR-II Mk-III) was created. This configuration will require a steel-sodium reflector element below the beam tube on the open side of the "C." For present survey purposes, pure sodium was used.

6.2 Results

It was found, as shown in Table 6.1, that this neutronically leaky core could provide the necessary thermal power. These results suggest that reactivity compensation for burnup losses could be accomplished by periodically increasing the reflector size, rather than by increasing the core size, which would undesirably reduce the core average power density.

Table 6.1 Effect of Target Vertical Location on Power

Beam fixed at 5 MW; 98 fuel assemblies; 113 reflector assemblies; inclined beam

Beam Axis offset, cm	*Power, MWt*
-4.0	*104.4*
-2.0	*106.1*
-1.2	*107.9*
-1.0	107.6
105.6	
+2.0	102.5
+6.0	91.2

It is clear from Table 6.1 that the system power has a maximum near an offset of only –1.2 cm. It is surprising that the geometrical center so closely matches the neutronic center. It is also clear from Table 6.1 that mismatching the target can significantly reduce the system power.

Table 6.2 presents information concerning the relative axial power distribution for a series of cases in which an axial offset of –1.0 cm was taken as the "best" nominal dimension. Axial power shape information for EBR-II was obtained from Golden and Miller [8]. Fig. 7 of that

reference shows the axial fission rate distribution for U-235, averaged over Runs 24, 27A, and 31F. The profile was approximately fitted to an equation of the form:
$P = A \cos[B(x-x0)]$,
where x ranges from 0-1 and x0 is 0.48. The power peak is displaced slightly toward the bottom. Note that x=0 is the bottom, and x=1 is the top. B is about 1.447 radians. Upon integrating this fit, the powers in the top third, middle third, and lower third of the core are about 31.5%, 36.1%, and 32.4%. The axial peak/average power ratio is 1.093. From Table 6.2, one can see that the axial power profile in the SCM-100 is quite flat, and is slightly peaked toward the bottom of the core, just as in EBR-II. Even though the axial segmentation for the comparison to MCNPX calculations is only in thirds, it is clear that the axial power profile is very nearly that of a critical system without a neutron source, such as existed in EBR-II. It is concluded that power peaking considerations axially are very nearly the same as in EBR-II. The axial power profile is dominated by the fission source, which is influenced by the presence of axial neutron reflectors. This result is expected because the neutron multiplication is quite high.

Table 6.2 Relative Power in the Top, Middle, and Bottom Thirds of the Active Fuel of the SCM-100

No. of Reflector Assemblies	P(top), %	P(middle), %	P(bottom), %	Total MWt
0	30.32	36.54	33.14	28.97
41	30.50	36.44	33.06	48.24
84	30.68	36.37	32.95	78.00
113	30.82	36.32	32.87	107.60
135	30.84	36.32	32.84	127.70

Radial power peaking factors are difficult to determine by probabilistic methods such as are used by MCNPX. However, some useful information was obtained by grouping fuel elements into small clusters. Fuel element locations were characterized as shown in Table 6.3. Clusters 1, 3, 4, and 5 are in the beam path, with 1 closest to the beam. Clusters 6, 7, and 8 are the rows on each side of the beam, with 6 closest to the beam. The predicted radial peak/average power ratio for these groups of fuel assemblies is 1.563/0.726 or 2.15. For comparison, the EBR-II radial power peaking factor was 1.46. These results do not have sufficient spatial detail to find the subassembly with the most power. Neither has the core arrangement been optimized to reduce radial power peaking. However, they are a clear indication that radial power peaking of the "C"-shaped core (that is necessary for the inclined entry beam) is a design issue. It is probably a key disadvantage of this concept, relative to a vertical entry design. Although these conclusions were obtained using EBR-II Mark-IIIA fuel elements of a single enrichment, they are expected to be true for any single-enrichment fuel design with a similar active fuel height and similar k-infinity.

Table 6.3 Groupings of Fuel Assemblies in the MCNPX Model

98 fuel assemblies; 113 reflector assemblies; inclined entry

Cluster	Number of Fuel Assemblies	Location	Avg. Power, MWt
1	11	column 1 (innermost)	0.963
3	11	column 2	1.563
4	13	column 3	1.455
5	15	column 4	1.263
6	16	row 1 (innermost)	0.843
7	16	row 2	0.817
8	16	row 3	0.726

6.3. Summary and Conclusions for the Inclined Entry SCM-100

It is clear that the k-effective can be varied over a wide range just by varying the reflector thickness. Obtaining 100 MWt in conjunction with a 5 MW beam is readily obtained using standard EBR-II fuel assemblies of nominal enrichment (~67%). A core containing 98 fuel assemblies and 113 reflector elements will provide 107.6 MWt from a fresh, unburned core. Power changes with burnup can be compensated by changing the beam power, by fuel assembly reshuffling, and by adjusting the reflector. Power peaking axially is not very different from that of EBR-II. Radial power peaking of configurations that were modeled is excessive compared to EBR-II, and therefore is a key design constraint.

Table 6.4 Effect of Beam Source vs. Fission Source on Power

Inclined Entry, Steel/Sodium Reflector Above and Below Beam Tube

Description	k-eff Fission Source	Power, Mwt Beam Source	Predicted Power from k-eff and Fission Source at 99% conf., MWt
No radial reflector	0.84402+/-0.0057	29.69	31.7-32.4
41 reflector elements	0.90682+/-0.00062	48.41	52.73-54.62
84 reflector elements	0.94130+/-0.00062	78.86	82.87-87.61
113 reflector elements	0.95704+/-0.00062	105.6	112.13-120.98
135 reflector elements	0.96050+/-0.00063	120.5	121.45-132.17

7. References

1. J. Herceg, “Accelerator-Driven Test Facility: Subcritical Multiplier (SCM-100) Station System Design Description,” Private Communication, ANL Report to be published in 2002.
2. L. J. Koch et al., “Hazard Summary Report, Experimental Breeder Reactor II (EBR-II), ANL-5719, Argonne National Laboratory, May 1957.
3. S.A. Kamal, “An Overview of LMR In-Vessel Radial Shield Designs, ANL-FRA-162, Argonne National Laboratory, March 1988.
4. M. Grotenhuis, A. E. McArthy, and A. D. Rossin, Experimental Breeder Reactor-II (EBR-II) Shield Design, ANL-6614, Argonne National Laboratory, September 1962.
5. R.M. Fryer, G.L. Batte, R.C. Brubaker, L.K. Chang, R.W. King, J.F. Koenig, D.L. Porter, W.H. Radke, J.H. Smith, and G.C. Wolz, unpublished information, Argonne National Laboratory, May 1992.
6. IPNS UPGRADE: A Feasibility Study, ANL-95/13, Argonne National Laboratory, April 1995.
7. RSICC Computer Code Collection, MCNPX 2.1.5, CCC-705, Oak Ridge National Laboratory, Radiation Safety Information Computational Center, August 2000.
8. G. H. Golden and L. B. Miller, “Method for Calculating Distributions of Flux, Power, and Burnup in Oxide Subassemblies Irradiated in EBR-II,” ANL-7880, Argonne National Laboratory, 1972.